Innovative Application of Artificial Neural Networks for Effective Rotational Shaft Crack Localization

Salah Mahmood Shakir
Mechanical Engineer
Ministry of Finance
Administrative and Financial Engineering Department
Mechanical Engineering Department
University of Technology- Iraq
Baghdad
Iraq

Alaa Abdulhady Jaber
Assistant Professor (PhD)
Mechanical Engineering Department
University of Technology- Iraq
Baghdad
Iraq

Rotational shafts are pivotal components in industrial settings and are responsible for transmitting torque and rotational motion. Despite their significance, these shafts are susceptible to faults, particularly cracks, which can adversely affect the system's performance and safety. Hence, efficient crack detection and diagnosis ensure safety, reliability, and cost-effectiveness. This research aims to develop an Artificial Neural Network (ANN) model that can effectively identify cracks occurring at different depths and locations in rotating shafts, which operate at varying rotational speeds. Vibration signals were obtained and subjected to preprocessing using a bandpass filter to isolate the shaft signals from other components. Subsequently, time-domain statistical features were extracted from the filtered signals. An optimal feature selection methodology was employed to rank the extracted features, and the highest-ranking features were chosen for training the ANN model. The findings of this research indicate that the developed model achieved a classification accuracy of 94.4%.

Keywords: *Artificial Neural Network, Crack Detection, ReliefF, Signal Processing, Vibration Analysis.*

1. INTRODUCTION

Rotating shafts play a critical role as essential components in various industries where alternating loads are encountered, such as power plants, generators, compressors, aircraft engines, and wind turbines. These shafts are subjected to continuous rotation and are responsible for transmitting torque and rotational motion within the respective machinery. However, despite their vital function, rotating shafts are prone to various types of failures throughout their operational lifespan. These failures include misalignment or unbalance during the installation process, as well as the development of cracks, erosion, and wear during regular operation. The occurrence of such faults can have detrimental consequences, leading to diminished performance, equipment failure, and imposing significant financial burdens for repair or replacement. Under extreme operating conditions and subjected to repeated loads, rotating shafts are susceptible to local plastic deformation, which can give rise to surface flaws. Over time, these initial flaws have the potential to propagate and develop into cracks. When the stress intensity factors at the crack front exceed the critical stress intensity factor, the crack may undergo rapid propagation. This phenomenon can ultimately lead to catastrophic fatigue crack failure, posing significant risks and potential dangers [1]. Despite their typical ductile nature, they can exhibit brittleness in fatigue fractures formed by cracks. Consequently, the early detection of cracks in rotor systems has become a matter of growing concern for engineers and researchers [2], [3]. Detecting and diagnosing shaft cracks in rotor systems is crucial to preventing catastrophic failures, maintaining equipment reliability, and protecting personnel safety.

Currently, vibration-based fault detection is considered a practical and effective approach for diagnosing mechanical equipment [4]. According to research by Malla and Panigrahi [5], vibration-based condition monitoring has been found to be highly successful in detecting machine faults or failures, with the capability of identifying up to 90% of such issues. This is because each component within a system or device possesses a specific vibration signature closely associated with the machine's operating conditions. Rotating machines typically consist of multiple components, such as shafts, bearings, pumps, gears, and fans. Any damage or failure to these components leads to abnormal vibrations compared to normal operational conditions. Complex vibration data is acquired from rotating machine components through signal processing techniques, which help resolve noise elimination, demodulation, and analysis issues and enhance technology for feature extraction when analyzing vibration signals from rotating machinery. Features of monitored signals are extracted using signal processing techniques to eliminate redundant information and analyze the corresponding patterns in the time and frequency domains and nonlinear features [6], [7]. Features play a crucial role in fault detection in rotating machinery. Statistical features such as mean, standard deviation, skewness, and kurtosis are utilized to describe the overall features of the vibration signal, but they are limited in their ability to detect changes in the signal.

On the other hand, frequency-domain features, including energy, power spectral density, and root mean

Received: September 2023, Accepted: December 2023
Correspondence to: Alaa Abdulhady Jaber
Mechanical Engineering Department,
University of Technology- Iraq, Baghdad, Iraq,
alaa.a.jaber@uotechnology.edu.iq
doi: 10.5937/fme2401103S

square, are derived from the Fourier transform of the signal and are highly sensitive to changes in the mecha–nical system, including shifts in natural frequency, damping, and stiffness, which are often indicative of damage or failure. Time-domain features, such as the time signal and its derivatives, and statistical para–meters, such as mean, variance, and peak-to-peak value, are useful for the early detection of faults. The choice of fault diagnosis features depends on the fault type and the application's specific needs. The application of appropriate features can significantly enhance the accu–racy and reliability of fault diagnosis in rotating mac–hinery. However, it is not possible to identify fault patterns by directly removing features. Hence, the utilization of these characteristics in machine learning and artificial intelligence techniques is necessary to enable the categorization of faults. In the diagnosis of rotating equipment, classifiers and statistical learning approaches have been widely used, such as Artificial Neural Networks (ANN) [8-11], K-Nearest Neighbor (k-NN)[12–14], Decision Tree (DT) [15-17], Support Vector Machine (SVM) [18-21], and other algorithms.

Various studies have been conducted on rotating shaft fault diagnosis, providing valuable contributions and insights. Guan et al. [22] proposed two dynamic model variations to address shaft misalignment. Then, these models were subjected to both simulation and experimental evaluations. Bovsunovsky [23] presented a methodology that employs the principles of linear fracture mechanics to calculate the relative change in the compliance of a shaft caused by the presence of a crack. Huo et al. [24] presented a study that evaluated the performance and efficiency of crack fault detection through the utilization of wavelet packet decomposition (WPD) and empirical mode decomposition (EMD) in combination with multiscale entropy (MSE) for the diagnosis of rotating shaft faults. Gradzki et al. [25] proposed a novel signal-based methodology for detec–ting cracks in rotors utilizing auto-correlation and power spectral density functions derived from the vibration signals acquired at the bearings of the rotating shaft. Jeon et al. [26] created a noncontact method for iden–tifying fatigue cracks in rotating steel shafts using air-coupled transducers. The method's efficacy was eva–luated through experiments using ultrasonic data on real fatigue cracks on half-scale and full-scale steel shafts used in automobile assembly lines subjected to cyclic loading tests. Azeem et al. [27] employed a method of order analysis to detect misalignment and shaft cracks. The time-domain data obtained were transformed into spectra utilizing a Fast Fourier Transform (FFT), which was then used to conduct the order analysis in real-time. Sinou [28] studied the possible connections between nonlinear vibrations and the occurrences of higher-order antiresonances and structural modifications resulting from breathing cracks in rotor systems. In the context of using AI for fault classification, Jiang et al. [29] proposed a diagnostic method for faults in rotating machinery that employs the fusion of multi-sensor information, where all features are derived from vibration data in the time domain to form a fusion vector, and the SVM is utilized for classification. Rahmoune et al. [30] proposed a predictive control strategy for the high-pressure shaft speed of a gas turbine using ANN to monitor the vibratory behavior of the rotating machine. Yan et al. [31] presented a new algorithm for multi-sensor data fusion that utilizes the K-nearest neighbor classification method to identify im–balance, misalignment, and rub-impact in rotating machinery. Umbrajkaar et al. [32] employed a combi–nation of ANN and SVM for the classification and assessment of shaft misalignment under varying load conditions. Zhao et al. [30] presented a method of fault diagnosis that employs a multi-input convolutional neural network (MI-CNN) was presented by Zhao et al. [33] for the classification of shaft misalignment and cracks in rotor systems. Liu Zhao et al. [34] proposed a novel method for diagnosing unbalance, misalignment, and contact-rubbing in rotating shafts based on the use of a convolutional neural network (CNN), discrete wavelet transform (DWT), and singular value decom–position (SVD). Seplveda and Sinha [35] proposed a smart vibration-based machine learning model (SVML) to diagnose rotor failures, including misalignment, shaft bow, looseness, and rubbing. Gangsar et al. [36] pro–posed a new approach to improve the accuracy of diagnosing unbalanced faults in rotating machinery using an SVM in combination with both time and frequency domains. Lee et al. [37] proposed a strategy for detecting shaft misalignment defects in rotating machinery through the use of an SVM for fault recognition, which was based on the analysis of the values of the components of the power spectrum in the frequency domain classified by the principal component analysis (PCA). Rao [38] utilized a combination of ANN and wavelet transforms to detect irregularities, such as open cracks or grooves on a rotating stepped shaft with multiple discs. Zamorano et al. [39] created a technique for choosing the mother wavelet in the wavelet packet transform method to improve the detection of cracks in rotating elements through SVM.

While examining the existing literature, it becomes apparent that the predominant focus of prior investi–gations in this field has centered on fundamental signal analysis. However, a notable gap contributing to in–consistent results and diminished accuracy in machine learning classifiers arises from the direct utilization of features extracted from signals without an intermediate preprocessing step. The absence of such preprocessing, involving techniques like noise reduction, filtering, or normalization, poses potential risks by introducing noise, distortions, or inconsistencies in the feature data. This directly impacts the performance and accuracy of machine learning classifiers. Thus, it is imperative to integrate suitable signal preprocessing techniques to mi–tigate these limitations and enhance the overall effec–tiveness of classifiers in analyzing and classifying vib–ration signals. To address these challenges, we advocate for robust signal preprocessing, specifically employing a bandpass filter applied to collected data. This critical preprocessing step significantly contributes to classifier performance enhancement and is, therefore, a crucial aspect of our proposed methodology. Furthermore, we underscore the paramount importance of feature selec–tion alongside signal preprocessing. Researchers must diligently identify the optimal feature combination that

captures and represents pertinent information within vibration signals, ultimately aiming for optimal results in terms of classification accuracy and overall performance.

This paper introduces an innovative application of ANN for detecting cracks in rotating shafts, critical components in various industries. The developed ANN model can identify cracks at different depths and loca–tions, contributing to enhanced equipment reliability, safety, and cost-effectiveness. The practical applications include proactive maintenance through early crack de–tection, leading to improved equipment longevity. The automated capabilities of the ANN model offer a cost-effective solution by reducing manual inspection efforts, saving time, and conserving resources.

In this paper, the development of an ANN model for the identification of crack depth and locations in rotating shafts operating at various rotational speeds is presented. To accomplish this objective, a test rig was designed and fabricated to provide a suitable platform for experimental investigations. Cracks of varying depths and locations were simulated in the shafts using a wire electrical discharge machine (WEDM). A data acquisition system was developed by integrating a micro-electromechanical system (MEMS) with data acquisition hardware and LabVIEW software. To improve the accuracy of the analysis, Bessel bypass filters were employed to filter the acquired vibration signals effectively. This filtering process successfully isolated the shaft vibration signals of interest, elimi–nating any extraneous signals originating from other components. Statistical features were derived from the filtered time-domain signals and subsequently utilized in the ReliefF feature ranking method. This method allowed for the identification of the most informative features. Finally, an AI classification model based on ANN was developed, incorporating the top-ranked features for the training of the model.

The remainder of this paper is organized as follows Section 2 presents a comprehensive overview of the experimental procedures, encompassing details regarding the test rig, crack simulation, as well as the data acquisition system and signal processing techniques employed. The process of extracting and selecting relevant features using the ReliefF algorithm is examined in depth in Section 3. The classification model employed in this investigation is elaborated upon in Section 4. In Section 5, the obtained results are presented and analyzed. Finally, the conclusions drawn from this study are summarized in Section 6.

2. EXPERIMENTAL STUDY

This section provides details of the experimental test rig used to detect and diagnose cracks in a rotating shaft, crack fault simulation, and the data acquisition system, including hardware and software.

2.1 Test Rig Design

An experimental test setup was specifically designed and fabricated to evaluate shafts with a diameter of 20 mm and a length of 500 mm, as illustrated in Figure 1. This test rig consisted of a 0.75 kW three-phase electric motor, which was controlled by a Hyundai N700E variable frequency drive (VFD). In order to minimize misalignment, a flexible coupling was utilized to estab–lish a connection between the shaft and the electric motor.

The experimental setup included a rotating disk with a diameter of 200 mm, a thickness of 35 mm, and a weight of 8 kg, which served as the load attached to the shaft. To ensure the secure placement of the accel–erometer, the top edge of the bearing housing was machined, drilled, and threaded. An ADXL335 three-axis accelerometer [40] was then mounted on the top edge of the bearing housing using two M3 bolts, guaranteeing its stability throughout the test operation.

2.2 Fault Simulation

This research encompassed the examination of an intact shaft (Healthy) in addition to nine shafts exhibiting cracks at different depths and locations, as presented in Table 1. These shafts were made of C45 carbon steel and measured 500 mm in length and 20 mm in diameter. The cracks were artificially simulated using a wire electrical discharge machine (WEDM) with a wire diameter of 0.25 mm and a cutting edge positioned at a 90-degree angle to the shaft's axis. Cracks were created at depths of 2 mm, 5 mm, and 8 mm, positioned at distances of 90 mm, 270 mm, and 410 mm from the edge of the shaft, respectively. Table 1 provides a comprehensive list of cases, while Figure 2-A visually depicts the shafts with simulated cracks. Additionally, Figure 2-B presents a side view showcasing the depths of the simulated cracks.

The case name for each experimental scenario was represented as a ratio of the crack depth to the crack loca–tion measured from the driven edge of the shaft. It is worth noting that the (Healthy) condition of the shaft, which was free of any cracks, was included as a reference point.

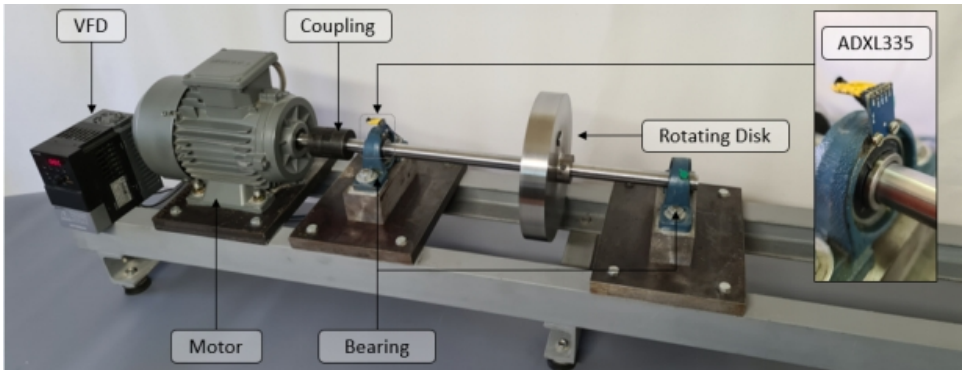

Figure 1. Experimental Test Rig

Table 1. Experimental cases.

Case Name	Distance from Shaft Edge	Depth	Distance from Sensor
Healthy	-	-	-
2/90	90 mm	2 mm	14 mm
2/270	270 mm		194 mm
2/410	410 mm		334 mm
5/90	90 mm	5 mm	14 mm
5/270	270 mm		194 mm
5/410	410 mm		334 mm
8/90	90 mm	8 mm	14 mm
8/270	270 mm		194 mm
8/410	410 mm		334 mm

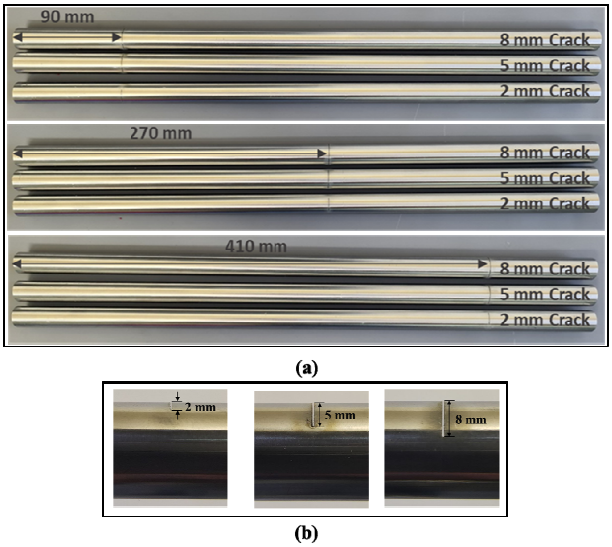

Figure 2. (a) Crack Simulations on Shafts (b) Side View

2.3 Data Acquisition System and Signal Preprocessing

To collect vibration data, the accelerometer was connected to a 16-bit NI USB-6215 data acquisition device (DAQ), as depicted in Figure 3. The LabVIEW software platform [41] was employed for signal processing and feature extraction.

The block diagram in Figure 4 illustrates the signal flow, starting with the DAQ Assistant and followed by manual calibration for the accelerometer. The LabVIEW Filter VI offers five different infinite impulse response (IIR) filter topologies: Butterworth, Chebyshev, Inverse Chebyshev, Elliptic, and Bessel. To determine the optimal topology, a comparison program was developed in LabVIEW, which ranked the Bessel topology as the most suitable choice with an 8th order. A Bessel bandpass filter was then applied to the vibration signal to capture the shaft frequency while suppressing irrelevant frequencies originating from other assembled components. Figure 5 illustrates the effects of filtering on the vibration signal in both the time and frequency domains, and the specific low cut-off and high cut-off frequencies corresponding to each rotational speed are provided in Table 2.

For every experimental case, time-domain signals were captured with a sampling frequency of 1600 Hz at three distinct rotational speeds: 1200, 1800, and 2400 rpm. In total, 800 samples were acquired at each speed for every case. From each filtered signal, five features were extracted from each axis, yielding a dataset with dimensions of 24000×15.

Table 2. Cut-off frequencies.

Rotation Speed (rpm)	Shaft Frequency (Hz)	Low Cut-off Frequency (Hz)	High Cut-off Frequency (Hz)
1200	20	19	21
1800	30	29	31
2400	40	39	41

3. FEATURE EXTRACTION AND SELECTION

In this research, a total of fifteen features were extracted from the filtered vibration signals obtained from each axis of the accelerometer. These features encompassed five statistical measures: Root Mean Square (RMS), Standard Deviation, Kurtosis, Skewness, and Crest Factor. The following provides a summary of these features along with their corresponding equations:

- Root Mean Square (RMS): is a statistical measure used to characterize the magnitude of a set of numeric values, calculated by taking the square of each value of the signal, finding the average of those squares, and then taking the square root of the average. RMS is commonly used to define a signal or waveform's overall power or energy.

$$RMS = \sqrt{\frac{1}{N}\sum_{i=1}^{N} x_i^2} \tag{1}$$

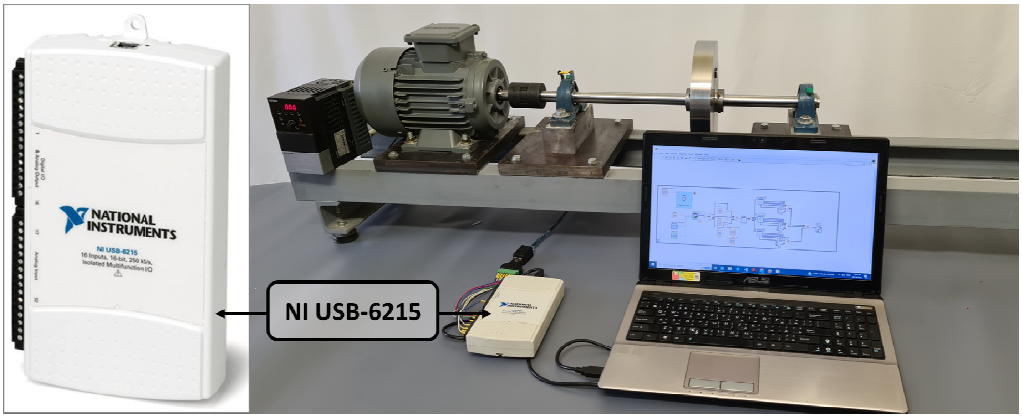

Figure 3. Data Acquisition Device

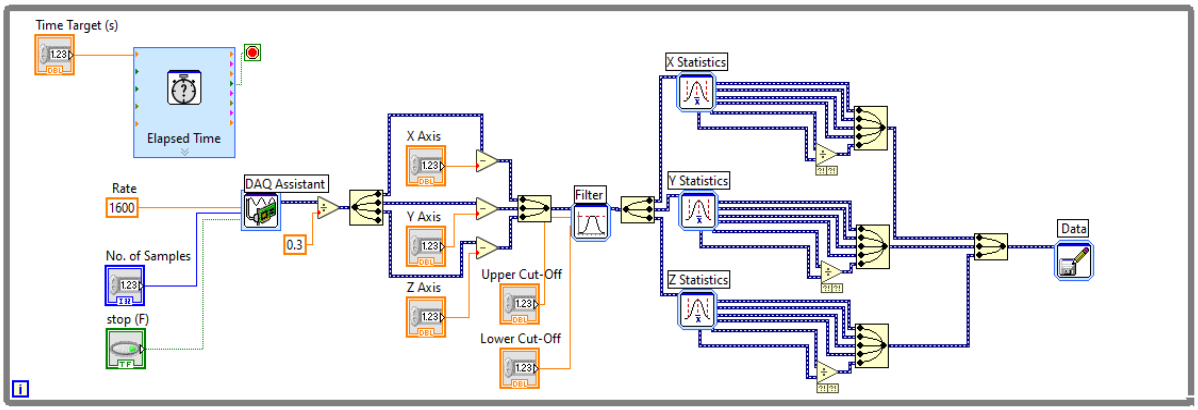

Figure 4. LabVIEW Block Diagram

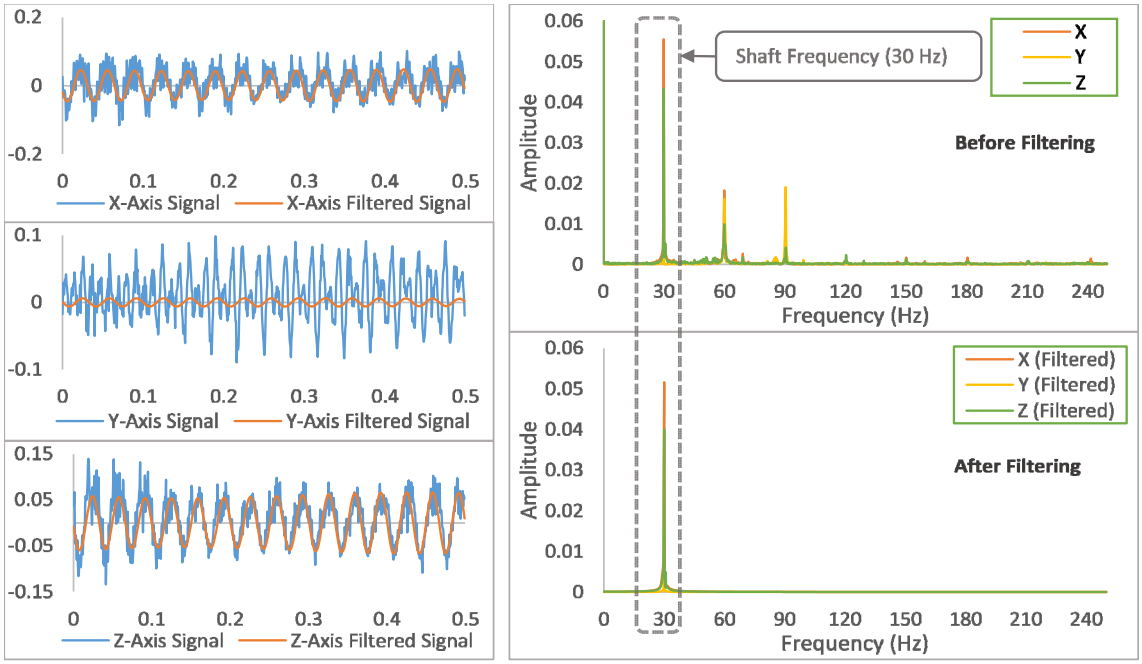

Figure 5. Filtering Effect on Vibration Signal at 1800 rpm

- Standard Deviation (STD) is a measure of the dispersion or spread of a distribution. It is calculated by taking the square root of the variance of a set of numbers. Standard deviation measures the amount of variation or dispersion in a data set and helps determine how close the values are to the mean or average value.

$$\mathrm{STD}(\sigma)=\sqrt{\frac{1}{N}\sum_{i=1}^{N}(x_i-\mu)^2} \tag{2}$$

- Crest Factor (CF): is a measure of the peak-to-average ratio of a waveform or signal. It is calculated by dividing the peak value of a signal by its RMS value. The crest factor is often used to assess the potential for audio and other signal distortion.

$$\text{Crest Factor (CF)} = \frac{V_{max}}{RMS} \tag{3}$$

- Kurtosis (K): is a measure of the peakedness of a distribution. A distribution with a high kurtosis has a more peaked shape than a normal distribution, while a distribution with a low kurtosis has a flatter shape.

$$\text{Kurtosis} = \frac{N\sum_{i=1}^{N}(x_i-\mu)^4}{\left[\sum_{i=1}^{N}(x_i-\mu)^2\right]^2} \tag{4}$$

- Skewness (Sk): is a measure of the asymmetry of a distribution. Skewness can be positive, negative, or zero. A distribution with positive skewness is skewed to the right, a distribution with negative skewness is skewed to the left, and a distribution with zero skewness is symmetrical.

$$\text{Skewness(Sk)} = \frac{N\sum_{i=1}^{N}(x_i-\mu)^3}{\sigma^3} \tag{5}$$

where xi is a signal for i = 1, 2,...,N. N is the number of data points, Vmax is the maximum value of (xi), μ is the signal value.

3.1 ReliefF Ranking Algorithm

The presence of a large number of features can pose challenges in the classification process, making it difficult to identify appropriate characteristics for classification purposes. Incorporating an excessive number of features can lead to increased operational complexity, reduced processing speed, and compro–mised classification accuracy, particularly when the available number of samples is limited [42]. In such scenarios, the utilization of feature selection or dimen–sionality reduction methods becomes imperative to facilitate the classification process. Among these met–hods, the ReliefF algorithm stands out as one of the most effective filtering feature selection techniques.

The Relief algorithm was first introduced by Kira in 1992 as a solution for two-class classification problems [43]. This algorithm assigns weights to features according to their correlation with the class labels and selects those features whose weights exceed a specified threshold. The correlation is measured based on the features' ability to differentiate between samples in close proximity. The Relief algorithm has gained popularity due to its simplicity, efficiency, and satisfactory results. However, a notable limitation of the Relief algorithm is its capability to handle only two-class classification problems. To address this limitation, Kononenko pro–posed the ReliefF algorithm in 1994 [44], which extends the functionality of the Relief algorithm to handle multiclass classification problems.

In the context of multiclass classification problems, the ReliefF algorithm adopts a process where a sample Ri is randomly selected from the training dataset with class labels represented as $C = \{c1, c2, \ldots, cl\}$. Subsequently, the algorithm identifies the k nearest neighbors of sample R_i that share the same class label (referred to as near Hits) and assigns them labels $H_j(c)$ (where $j = 1, 2, \ldots, k$). Additionally, the algorithm identifies the k nearest neighbors of Ri that belong to other classes (known as near Misses), denoted as $M_j(c)$ (where $j = 1, 2, \ldots, k$). These steps are repeated m times as part of the algorithm's execution [45]. The assigned weight of feature A is adjusted as follows:

$$W^{(i+1)}(A) = W^{i}(A) - \sum_{j=1}^{k} \frac{\mathrm{diff}(A, R_i, H_i)}{mk} + \frac{\sum_{c \notin class(R)} \left[\frac{p(c)}{1 - p(class(R))} \sum_{(j=1)}^{k} \mathrm{diff}(A, R_i, M_i(c)) \right]}{mk} \quad (6)$$

where m is the iteration number, and $\mathrm{diff}(A, R_1, R_2)$ represents the disparity between samples R_1 and R_2 in feature A. If A is continuous, the difference can be defined as:

$$\mathrm{diff}(A, R_1, R_2) = \frac{|R_1[A] - R_2[A]|}{\max(A) - \min(A)} \quad (7)$$

If A is discrete, then the *diff* can be defined as:

$$\mathrm{diff}(A, R_1, R_2) = \begin{cases} 0 & ; \quad R1[A] = R_2[A] \\ 1 & ; \quad R1[A] \neq R_2[A] \end{cases} \quad (8)$$

4. CLASSIFICATION MODEL

Artificial Neural Networks are computer structures ins–pired by the functioning of neurons in the human brain. The first ANN was created by the psychologist Frank Rosenblatt in 1958. [46]. An ANN is made up of a network of connected neurons that are stacked in layers. ANN typically comprises an input layer, an output layer, and at least one hidden layer. The number of input and output variables necessary to characterize the problem and its type determines the number of neurons in the input and output layers, while the trial-and-error approach decides the number of hidden layers and neurons between each layer. As illustrated in Figure 6, each neuron in a layer (except the input layer) adds the input value to the corresponding weight to generate a single threshold value. The single-value threshold is combined with a bias to obtain a net value (Net). Finally, an activation function is applied to the net value to provide an output value. A supervised learning technique compares the input and output values and then uses a backpropagation algorithm to train the ANN model by altering the weights between each neuron in the various layers [47]. Due to its superior performance, ANN has been used in many applications, including pattern identification, fault prediction and classification, voice recognition, handwritten and printed text recognition, and detection of heart disease and cancer detection [48-52].

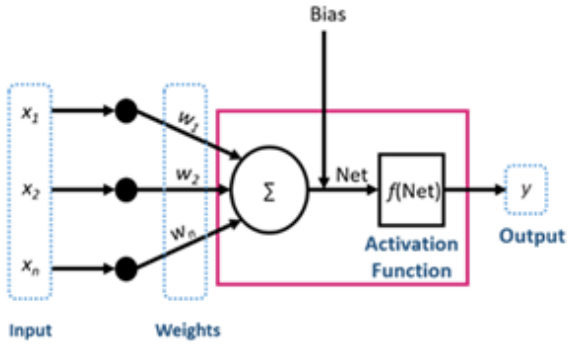

Figure 6. Artificial Neural Networks

4.1 Neural Network Mathematical Expression

The mathematical expression of an ANN model entails a sequential arrangement of interconnected compu–tational units referred to as neurons, which are struc–tured in layers. These neurons receive input, undergo computational operations, and generate an output. The network's input is represented by $x_i(n)$, the hidden layer output is represented by f, and the neural network's output is represented by $y_i(n)$. The weights connecting the input layer to the hidden layer and the hidden layer to the output layer are represented by w_{ij} and w_{jk}, respectively. The output vector of the hidden layer can be calculated using the following equation:

$$f = Q_j[\sum_{(i=1)}^{N} (w_{ij} x_i(n) + B_j)] \quad , \quad j = 1,2,...,D \quad (9)$$

where B_j is the threshold of neurons in the hidden layer, N is the number of inputs, D represents the number of neurons in the hidden layer, and Q is the hyperbolic acti–vation function in the hidden layer. Which is given by:

$$\tanh = \frac{e^{x} - e^{-x}}{e^{x} + e^{-x}} \quad (10)$$

While the time index n has been omitted for simplicity, the output of the final output layer can be calculated as:

$$y_i(n) = Q_k[\sum_{(i=1)}^{D}(w_{jk}f + B_k)] \quad , \quad k = 1,2,...,D \qquad (11)$$

where B_k is the threshold for the neuron of the output layer, and E is the number of neurons in the output layer. The output of the ANN may then be expressed as:

$$y_i(n)=Q_k[\sum_{(i=1)}^{D}(w_{jk}\left[Q_j[\sum_{(i=1)}^{N}(w_{ij}x_i(n)+B_j)]\right] + B_k)] \qquad (12)$$

4.2 Neural Network Model Design

Orange Data Mining Software [53] was utilized in this research to design the ANN model, whose data processing flows are presented in Figure 7. The development of the ANN model involved an iterative process of experimentation and parameter tuning, encompassing various aspects such as the number of layers, neurons, solver, and activation function. Initially, a preliminary version of the ANN model was created with a single hidden layer and default parameter values. This initial model was then trained and evaluated to assess its classification accuracy. Subsequent iterations involved making several adjustments to enhance the performance of the ANN model. After multiple iterations, an optimal configuration was determined, which comprised four hidden layers, with 60, 40, 40, and 40 neurons allocated to each respective layer. Detailed information regarding the classifier's characteristics can be found in Table 3.

Table 3. ANN model properties.

Number of hidden layers	4
Neurons in the input layer	15
Neurons in the first hidden layer	60
Neurons in the second hidden layer	40
Neurons in the third hidden layer	40
Neurons in the fourth hidden layer	40
Neurons in the output layer	10
Activation function	RELU
Solver	Adam
Regularization (α)	0.0001
Maximum number of iterations	400

5. RESULTS AND DISCUSSION

This research employed an ANN approach to identify and diagnose the depth and location of cracks in rotating shafts operating at three different rotational speeds (1200, 1800, and 2400 rpm).

The experiment involved the investigation of an intact shaft alongside nine shafts with cracks at various depths and locations, as outlined in Table 1. The vibration data collected from the shafts were filtered and analyzed. Subsequently, five statistical features were extracted, and the ReliefF ranking algorithm was employed to designate the highest-ranked feature from each axis.

The ANN model received a dataset consisting of 2400 samples for each case, resulting in the formation of a matrix containing 24000 samples across 15 features. The data sampler allocated 80% of these samples for training the ANN model, with the remaining 20% reserved for testing the model.

The cases were examined under two distinct scenarios, denoted as S1 and S2. In Scenario S1, a total of fifteen features were obtained by extracting five time-domain features from the filtered vibration data associated with each accelerometer axis. These fifteen features were subsequently employed as input variables for the ANN model. In Scenario S2, the ReliefF ranking method was implemented on the feature set extracted from Scenario S1. This approach aimed to reduce the input feature dimensionality of the ANN model from fifteen to three. This reduction was accomplished by selecting the top-ranked features for each accelerometer axis based on their ReliefF scores.

The application of the ReliefF ranking method in this research demonstrated that the three highest-ranked features extracted were the root mean square values of the X, Y, and Z axes. Furthermore, the findings indicated that the filtering procedure resulted in the mean value becoming uniformly zero, leading to the RMS and STD features possessing identical values and, consequently, equivalent rankings. As a result, only the RMS feature was selected for further analysis. Figure 8 depicts the ranking and selection process of the extracted features.

The evaluation of a fault diagnosis system's performance can be accomplished by employing various performance indicators, including Classification Accuracy (CA), F1-Score, Precision (P), Recall (R), and Specificity [54]. These indicators offer a comprehensive system performance assessment by considering multiple aspects of the diagnosis process. The calculation of these performance indicators can be carried out using the following equations:

$$CA = \frac{T_P + T_N}{T_P + T_N + F_P + F_N} \qquad (13)$$

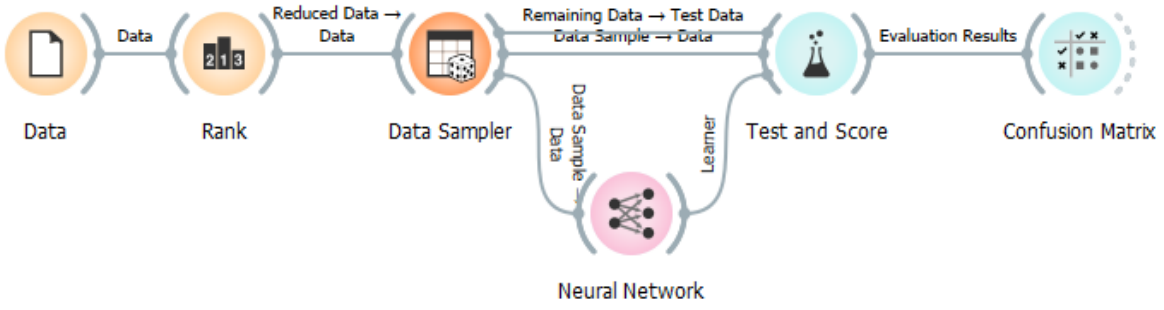

Figure 7. Data Processing Flow of ANN Model in Orange Data Mining

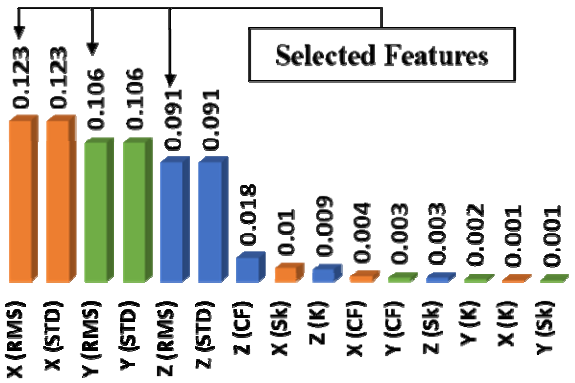

Figure 8. ReliefF Features Ranking and Selection for S2

$$F1 = \frac{2T_P}{2T_P + F_P + F_N} \tag{14}$$

$$Precision = \frac{T_P}{T_P + F_P} \tag{15}$$

$$Recall = \frac{T_P}{T_P + F_N} \tag{16}$$

$$Specificity = \frac{T_N}{T_N + F_P} \tag{17}$$

Table 4 illustrates the performance metrics of both S1 and S2 models. Under S1, utilizing all features extracted from vibration data, the ANN achieved a classification accuracy of 81.46%, F1 Score of 81.13%, Precision of 81.11%, Recall of 81.46%, and Specificity of 97.94%. These metrics collectively reflect the model's proficiency in accurately categorizing intact and cracked shaft instances.

Table 4. Performance matrices for both scenarios

Scenario	CA	F1	Precision	Recall	Specificity
S1	81.46%	81.13%	81.11%	81.46%	97.94%
S2	92.19%	92.16%	92.17%	92.19%	99.13%

Conversely, S2, incorporating the ReliefF algorithm, showcased substantial performance enhancement. It demonstrated higher Classification Accuracy (92.19%), F1 Score (92.16%), Precision (92.17%), Recall (92.19%), and Specificity (99.13%) compared to S1. The superior performance of S2, leveraging a more refined feature set, is evident across all evaluated parameters.

The outcomes underscore the importance of meticulous feature selection in optimizing ANN models for crack detection in rotating shaft applications. Specifically, the selective feature integration facilitated by the ReliefF algorithm signifies considerable advancements, emphasizing its potential to enhance the dependability and precision of crack detection systems in rotating machinery.

The performance of ANN in both scenarios is illustrated through the presentation of a confusion matrix, as depicted in Figures 9 and 10. The rows and columns of the matrix correspond to the actual and predicted instances, respectively. The instances that have been accurately classified are displayed along the diagonal of the confusion matrix. It is noteworthy that a total of 480 samples were employed for testing each case, resulting in an aggregate of 4800 samples.

The confusion matrix of the S1 model, as illustrated in Figure 9 and utilizing an ANN model trained with all the extracted features, demonstrates relatively good accuracy in classifying intact shaft (Healthy) from the cracked shafts, with 342 samples correctly classified. However, 95 of the samples were misclassified as 2/270. This suggests that the model effectively distinguishes intact shafts with a small error rate of 2/270, where this particular case involves a 2mm crack in the midspan. Moreover, 68 instances of 2/270 and 23 instances of 8/270 were erroneously classified as Healthy.

However, challenges arise when classifying cracked shafts, particularly in discerning between different crack depths and locations. Notably, the 2/90 case exhibits significant misclassification rates, with 156 of the samples classified as 5/270 and 103 of the samples as 8/90. Additionally, 116 instances from the 5/270 category were misclassified as 2/90. These findings suggest limitations in accurately determining specific crack configurations. The highest accuracy for cracked shafts is achieved in the 8/410 case, with 98.3% correctly classified (472 of 480 samples). Consequently, there are opportunities to improve the model's performance, which could be addressed through feature selection.

In contrast, the S2 model, as shown in Figure 10, incorporates the ReliefF feature selection algorithm, demonstrating improved performance compared to S1. ReliefF ranks the extracted features, and the top-ranked features from each axis are selected as input for the ANN. Results indicate enhanced accuracy in classifying intact shafts from the cracked shafts, with 397 samples correctly identified. Notably, the S2 model performs better in accurately classifying crack depths and locations than S1. For instance, the correctly classified samples of the 2/90 were improved from 221 in S1 to 404 samples in S2. This enhancement suggests that the ReliefF algorithm effectively identifies informative features for crack detection. Furthermore, the 8/410 case again achieves the highest accuracy, with 100% correctly classified. These results highlight the efficacy of ReliefF in selecting relevant features, contributing to improved crack detection in the S2 model.

A comparative analysis between the S1 and S2 models highlights the superior performance of the latter in terms of overall accuracy and precise classification of crack depths and locations. The incorporation of the ReliefF algorithm for feature selection in the S2 model leads to significant advancements. The S2 model demonstrates higher accuracy in classifying both the healthy and cracked shaft classes. Furthermore, it exhibits improved accuracy in accurately identifying specific crack configurations, as evidenced by the enhanced classification accuracy observed in the 2/90 case. These findings emphasize the effectiveness of the ReliefF algorithm in selecting relevant features, thereby contributing to enhanced crack detection performance. Consequently, the results suggest that feature selection plays a crucial role in enhancing the accuracy and robustness of crack detection models, demanding further investigation and refinement to achieve optimal performance.

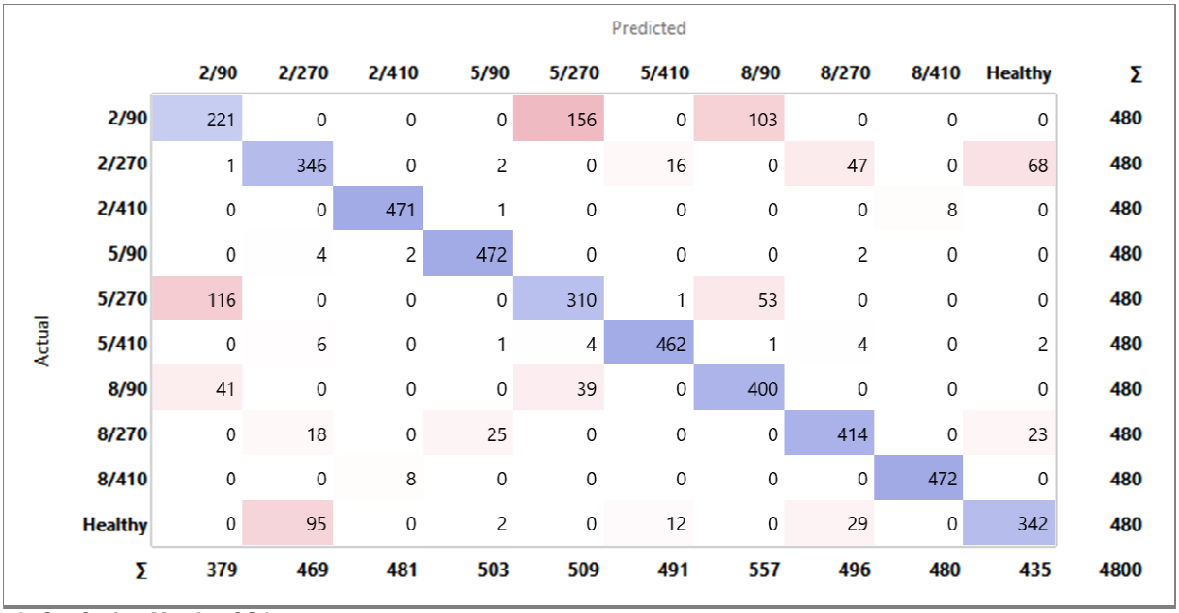

Figure 9. Confusion Matrix of S1

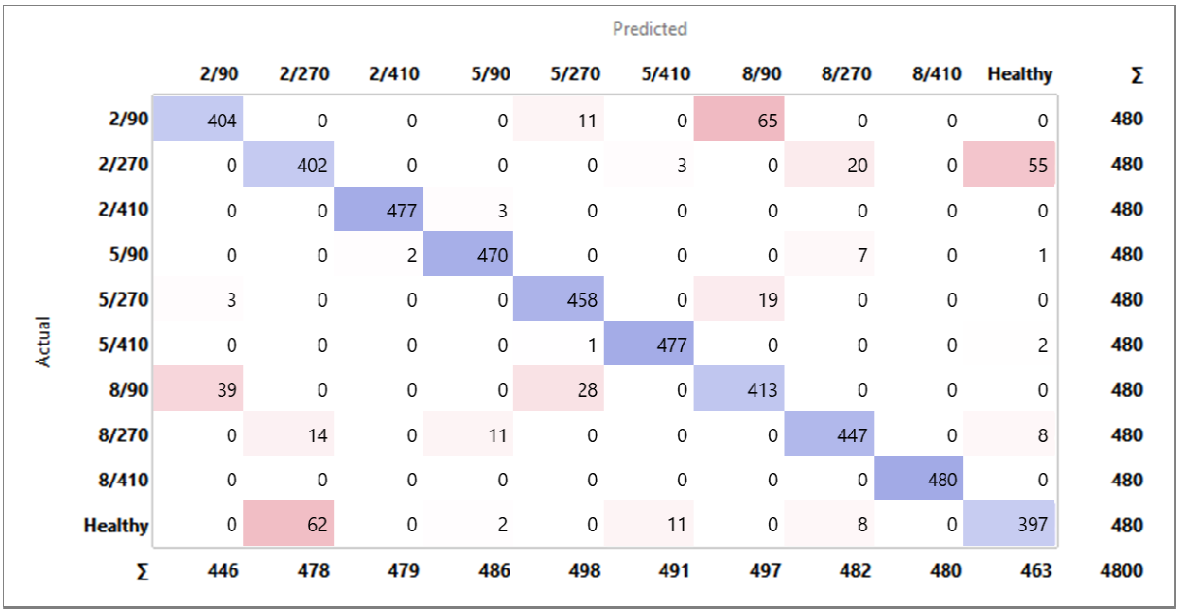

Figure 10. Confusion Matrix of S2

6. CONCLUSIONS

This study constitutes a noteworthy progression in the domain of crack detection within rotating shafts, employing a meticulous evaluation of two artificial neural network models, S1 and S2. The focal point on feature selection techniques has yielded pivotal insights into augmenting the precision and efficacy of crack detection models.

The outcomes of this inquiry underscore a notable limitation in S1. While demonstrating commendable performance in discerning intact shafts, it encountered impediments in accurately categorizing diverse crack depths and locations. This limitation accentuates the imperative for further refining crack detection models to heighten their efficacy.

Conversely, the integration of ReliefF feature selection in S2 has manifested as a substantial enhancement. Notably, S2 surpassed S1 by attaining superior overall accuracy and refined classification of crack depths and locations. This achievement substantiates the effectiveness of ReliefF in discerning informative features, thereby contributing to the advancement of crack detection methodologies.

A distinctive facet of this study, which sets it apart from previous endeavors, is the incorporation of filtered vibration signals in the analysis. Notably, a substantial number of earlier studies did not harness the potential of filtered signals, which our findings suggest can lead to a considerable improvement in results. This underscores the importance of incorporating such signal-filtering methodologies in future investigations, highlighting an avenue for further refinement.

The scholarly contribution of this study lies in its illustration of ReliefF's efficacy in refining machine-learning models for crack detection in rotating shafts, especially when utilizing filtered vibration signals. Through tangible enhancements in accuracy and classification, this research establishes a foundational framework for prospective investigations.

Furthermore, the findings underscore the potential for ongoing exploration and refinement of feature selection methods, coupled with the integration of sophisticated machine learning algorithms. The proposal to explore diverse sensor modalities and employ data fusion techniques in conjunction with filtered vibration signals represents an additional avenue for enriching the comprehensiveness of crack detection assessments.

Fundamentally, this study not only contributes to the understanding of crack detection in rotating machinery but also sets a standard for engineers and researchers seeking to improve proactive maintenance strategies and operational efficiency. The showcased advancements create opportunities for subsequent investigations, laying the foundation for ongoing innovation in the field of reliability within rotating machinery.

In conclusion, the developed ANN model holds significant practical implications across industries. Its application promises enhanced equipment reliability through proactive maintenance, contributing to improved safety and optimized performance. The model's adaptability and automated crack detection capabilities offer cost-effective solutions by reducing manual inspection efforts, saving time, and conserving resources. Ultimately, this research provides a valuable tool for pre-emptive maintenance, ensuring the longevity and efficiency of rotating machinery in diverse industrial contexts.

NOMENCLATURE

A	Feature in the ReliefF algorithm
Bj	Threshold of neurons in the hidden layer
Bk	Threshold of neurons in the output layer
C	Set of class labels {c1, c2, …, cl}
D	Number of neurons in the hidden layer
E	Number of neurons in the output layer
F_N	False negative values
F_P	False positive values
$H_j(c)$	Labels of k nearest neighbors with the same class label
$M_j(c)$	Labels of k nearest neighbors with other class labels
N	Number of data points
Q	Hyperbolic activation function in the hidden layer
Ri	Randomly selected sample from the training dataset
RMS	Root mean square
Sk	Skewness
Vmax	Maximum value of (xi)
diff(A, R1, R2)	Disparity between samples R1 and R2 in feature A
f	Hidden layer output
k	Number of nearest neighbors
m	Iteration number in the ReliefF algorithm
μ	Signal value
T_N	True negative values
T_P	True positive values
w_{jk}	Weights connecting hidden layer to output layer
w_{ij}	Weights connecting input layer to hidden layer
x_i	Neural network's input
y_i	Neural network's output

REFERENCES

[1] R. Alderliesten, “Fatigue crack propagation,” Solid Mech. its Appl., vol. 236, no. 5, pp. 175–220, 2017, doi: 10.1007/978-3-319-56227-8_9.

[2] O. Matsushita, M. Tanaka, H. Kanki, M. Kobayashi, P. Keogh, Vibrations of Rotating Machinery, vol. 2, no. 805. Springer, 2018. Available: http://link. Springer.com/10.1007/978-4-431-55456-1

[3] L. Vinet, A. Zhedanov, “A ‘missing’ family of classical orthogonal polynomials,” Journal of Physics A: Mathematical and Theoretical, vol. 44, no. 8. Universidade de São Paulo, p. 256, 2011. doi: 10.1088/1751-8113/44/8/085201.

[4] P. Tavner, L. Ran, J. Penman, and H. Sedding, “Condition monitoring of rotating electrical mac–hines,” Cond. Monit. Rotating Electr. Mach., vol. 2, no. 4, pp. 1–250, 2008, doi: 10.1049/ PBPO056E.

[5] C. Malla, I. Panigrahi, “Review of Condition Monitoring of Rolling Element Bearing Using Vibration Analysis and Other Techniques,” J. Vib. Eng. Technol., vol. 7, no. 4, pp. 407–414, 2019, doi: 10.1007/s42417-019-00119-y.

[6] Z. Huo, Y. Zhang, Z. Zhou, and J. Huang, "Crack detection in rotating shafts using wavelet analysis, Shannon entropy and multiclass SVM," in Lecture Notes of the Institute for Computer Sciences, Social-Informatics and Telecommunications Engi–neering, LNICST, 2018, vol. 221, pp. 332–346. doi: 10.1007/978-3-319-74176-5_29.

[7] P. Karolczak, “Application of Discrete Wavelet Transform to Analysis of Cutting Forces in Turning of Composites based on Aluminium Alloys Reinforced with Al2O3 Fibres,” FME Trans., vol. 49, no. 3, pp. 563–574, 2021, doi: 10.5937/fme2103563K.

[8] A. A. Jaber and R. Bicker, “Fault diagnosis of industrial robot bearings based on discrete wavelet transform and artificial neural network,” Int. J. Progn. Heal. Manag., vol. 7, no. 2, pp. 179–186, 2016, doi: 10.36001/ijphm.2016.v7i2.2365.

[9] D. Siano and M. A. Panza, “Diagnostic method by using vibration analysis for pump fault detection,” in Energy Procedia, 2018, vol. 148, pp. 10–17. doi: 10.1016/j.egypro.2018.08.013.

[10] A. Yunusa-Kaltungo and J. Sinha, “Generic vibration-based faults identification approach for identical rotating machines installed on different foundations,” Vib. Rotating Mach., no. 5, pp. 499–510, 2016.

[11] R. Vimal Sam Singh, A. Ramachandran, A. Selvam, and K. Subramanian, “Python inspired Artificial Neural Networks Modeling in Drilling of Glass-Hemp-Flax Fiber Composites,” FME Trans., vol. 49, no. 2, pp. 422–429, 2021, doi: 10.5937/ fme2102422S.

[12] M. Gohari and A. M. Eydi, “Modelling of shaft unbalance: Modelling a multi discs rotor using K-Nearest Neighbor and Decision Tree Algorithms,”

Meas. J. Int. Meas. Confed., vol. 151, p. 107253, 2020, doi: 10.1016/j.measurement.2019.107253.
[13] J. Lu, W. Qian, S. Li, and R. Cui, "Enhanced k-nearest neighbor for intelligent fault diagnosis of rotating machinery," Appl. Sci., vol. 11, no. 3, pp. 1–15, 2021, doi: 10.3390/app11030919.
[14] M. Altaf, T. Akram, M. A. Khan, M. Iqbal, M. M. I. Ch, and C. H. Hsu, "A New Statistical Features Based Approach for Bearing Fault Diagnosis Using Vibration Signals," Sensors, vol. 22, no. 5, Mar. 2022, doi: 10.3390/s22052012.
[15] V. Gunasegaran and V. Muralidharan, "Fault Diagnosis of Spur Gear System through Decision Tree Algorithm Using Vibration Signal," 2019. doi: 10.1016/j.matpr.2020.03.283.
[16] E. C. Yuvaraju, L. R. Rudresh, and M. Saimurugan, "Vibration signals based fault severity estimation of a shaft using machine learning techniques," Mater. Today Proc., vol. 24, pp. 241–250, 2020, doi: 10.1016/j.matpr.2020.04.273.
[17] S. Basangar and B. N. Tripathi, "Literature review on fault detection of equipment using machine learning techniques," Proc. Int. Conf. Comput. Autom. Knowl. Manag. ICCAKM 2020, pp. 62–67, 2020, doi: 10.1109/ICCAKM46823.2020.9051543
[18] B. Pang, G. Tang, C. Zhou, and T. Tian, "Rotor fault diagnosis based on characteristic frequency band energy entropy and support vector machine," Entropy, vol. 20, no. 12, p. 932, 2018, doi: 10.3390/e20120932.
[19] S. Suresh and V. P. S. Naidu, "Vibration Analysis of Heterogeneous Gearbox Faults using EMD Features and SVM Classifier," in IOP Conference Series: Materials Science and Engineering, Oct. 2019, vol. 624, no. 1. doi: 10.1088/1757-899X/624/1/012032.
[20] U. Parmar and D. H. Pandya, "Experimental investigation of cylindrical bearing fault diagnosis with SVM," Mater. Today Proc., vol. 44, pp. 1286-1290, 2021, doi: 10.1016/j.matpr.2020.11.327.
[21] D. P. Kumar, V. Muralidharan, and S. S. Hameed, "Multi-Point Tool Condition Monitoring System - A Comparative Study," FME Trans., vol. 50, no. 1, pp. 193–201, 2022, doi: 10.5937/fme2201193K.
[22] Z. Guan, P. Chen, X. Zhang, X. Zhou, and K. Li, "Vibration analysis of shaft misalignment and diagnosis method of structure faults for rotating machinery," Int. J. Performability Eng., vol. 13, no. 4, pp. 337–347, 2017, doi: 10.23940/ijpe.17.04.p1.337347.
[23] A. P. Bovsunovsky, "Efficiency analysis of vibration based crack diagnostics in rotating shafts," Eng. Fract. Mech., vol. 173, pp. 118–129, 2017, doi: 10.1016/j.engfracmech.2017.01.014.
[24] Z. Huo, Y. Zhang, and L. Shu, "A comparative study of WPD and EMD for shaft fault diagnosis," in Proceedings IECON 2017 - 43rd Annual Conference of the IEEE Industrial Electronics Society, 2017, vol. 2017-Janua, pp. 8441–8446. doi: 10.1109/IECON.2017.8217482.
[25] R. Gradzki, Z. Kulesza, and B. Bartoszewicz, "Method of shaft crack detection based on squared gain of vibration amplitude," Nonlinear Dyn., vol. 98, no. 1, pp. 671–690, 2019, doi: 10.1007/s11071-019-05221-0.
[26] I. Jeon, H. J. Lim, P. Liu, B. Park, A. Heinze, and H. Sohn, "Fatigue crack detection in rotating steel shafts using noncontact ultrasonic modulation measurements," Eng. Struct., vol. 196, no. February, p. 109293, 2019, doi: 10.1016/j.engstruct.2019.109293.
[27] N. Azeem, X. Yuan, H. Raza, and I. Urooj, "Experimental condition monitoring for the detection of misaligned and cracked shafts by order analysis," Adv. Mech. Eng., vol. 11, no. 5, pp. 1–11, 2019, doi: 10.1177/1687814019851307.
[28] J. J. Sinou, "Damage Detection in a Rotor Dynamic System by Monitoring Nonlinear Vibrations and Antiresonances of Higher Orders," Appl. Sci., vol. 12, no. 23, 2022, doi: 10.3390/app122311904.
[29] L. L. Jiang, H. K. Yin, X. J. Li, and S. W. Tang, "Fault diagnosis of rotating machinery based on multi-sensor information fusion using SVM and time-domain features," Shock Vib., vol. 2014, 2014, doi: 10.1155/2014/418178.
[30] M. Ben Rahmoune, A. Hafaifa, K. Abdellah, and X. Chen, "Monitoring of high-speed shaft of gas turbine using artificial neural networks: Predictive model application," Diagnostyka, vol. 18, no. 4, pp. 3–10, 2017.
[31] X. Yan, Z. Sun, J. Zhao, Z. Shi, and C. an Zhang, "Fault diagnosis of rotating machinery equipped with multiple sensors using space-time fragments," J. Sound Vib., vol. 456, pp. 49–64, Sep. 2019, doi: 10.1016/j.jsv.2019.05.036.
[32] A. M. Umbrajkaar, A. Krishnamoorthy, and R. B. Dhumale, "Vibration Analysis of Shaft Misalignment Using Machine Learning Approach under Variable Load Conditions," Shock Vib., Vol. 2020, 2020, doi: 10.1155/2020/1650270.
[33] W. Zhao, C. Hua, D. Wang, and D. Dong, "Fault Diagnosis of Shaft Misalignment and Crack in Rotor System Based on MI-CNN," in Lecture Notes in Mechanical Engineering, 2020, pp. 529–540. doi: 10.1007/978-981-13-8331-1_39.
[34] D. Liu, X. Lai, Z. Xiao, D. Liu, X. Hu, and P. Zhang, "Fault Diagnosis of Rotating Machinery Based on Convolutional Neural Network and Singular Value Decomposition," Shock Vib., vol. 2020, 2020, doi: 10.1155/2020/6542913.
[35] N. F. Espinoza Sepúlveda and J. K. Sinha, "Blind Application of Developed Smart Vibration-Based Machine Learning (SVML) Model for Machine Faults Diagnosis to Different Machine Conditions," J. Vib. Eng. Technol., vol. 9, no. 4, pp. 587–596, Jun. 2021, doi: 10.1007/s42417-020-00250-1.
[36] P. Gangsar, R. K. Pandey, and M. Chouksey, "Unbalance detection in rotating machinery based on support vector machine using time and frequency domain vibration features," Noise and Vibration Worldwide, vol. 52, no. 4–5. SAGE

Publications Inc., pp. 75–85, Apr. 01, 2021. doi: 10.1177/0957456521999836.
[37] Y. E. Lee, B. K. Kim, J. H. Bae, and K. C. Kim, "Misalignment Detection of a Rotating Machine Shaft Using a Support Vector Machine Learning Algorithm," Int. J. Precis. Eng. Manuf., vol. 22, no. 3, pp. 409–416, Mar. 2021, doi: 10.1007/s12541-020-00462-1.
[38] K. Babu Rao and D. Mallikarjuna Reddy, "Fault detection in rotor system by discrete wavelet neural network algorithm," JVC/Journal Vib. Control, vol. 28, no. 21–22, pp. 3315–3331, Nov. 2022, doi: 10.1177/10775463211030754.
[39] M. Zamorano, M. J. Gómez Garcia, and C. Castejón, "Selection of a mother wavelet as identification pattern for the detection of cracks in shafts," JVC/Journal Vib. Control, vol. 28, no. 21–22, pp. 3152–3161, 2022, doi: 10.1177/10775463211026033.
[40] M. H. Mohd Ghazali and W. Rahiman, "Vibration Analysis for Machine Monitoring and Diagnosis: A Systematic Review," Shock and Vibration, vol. 2021. Hindawi Limited, 2021. doi: 10.1155/2021/9469318.
[41] J. Kodosky, "LabVIEW," Proc. ACM Program. Lang., vol. 4, no. HOPL, pp. 1–54, Jun. 2020, doi: 10.1145/3386328.
[42] T. Blaschke, "Object based image analysis for remote sensing," ISPRS J. Photogramm. Remote Sens., vol. 65, no. 1, pp. 2–16, 2010, doi: 10.1016/j.isprsjprs.2009.06.004.
[43] K. Kira and L. A. Rendell, "The feature selection problem: Traditional methods and a new algorithm," in Aaai, 1992, vol. 2, no. 1992a, pp. 129–134.
[44] I. Kononenko, "Estimating attributes: Analysis and extensions of RELIEF," in Lecture Notes in Computer Science (including subseries Lecture Notes in Artificial Intelligence and Lecture Notes in Bioinformatics), 1994, vol. 784 LNCS, pp. 171–182. doi: 10.1007/3-540-57868-4_57.
[45] Z. Huang, C. Yang, X. Zhou, and T. Huang, "A hybrid feature selection method based on binary state transition algorithm and ReliefF," IEEE J. Biomed. Heal. informatics, vol. 23, no. 5, pp. 1888–1898, 2018.
[46] F. Rosenblatt, "The perceptron: A probabilistic model for information storage and organization in the brain," Psychol. Rev., vol. 65, no. 6, pp. 386–408, 1958, doi: 10.1037/h0042519.
[47] A. A. Jaber, "Design of an Intelligent Embedded System for Condition Monitoring of an Industrial Robot," Springer Nat., 2016, doi: 10.1007/978-3-319-44932-6.
[48] B. A. Paya, I. I. Esat, and M. N. M. Badi, "Artificial neural network based fault diagnostics of rotating machinery using wavelet transforms as a preprocessor," Mech. Syst. Signal Process., vol. 11, no. 5, pp. 751–765, 1997, doi: 10.1006/mssp.1997.0090.
[49] O. I. Abiodun, A. Jantan, A. E. Omolara, K. V. Dada, N. A. E. Mohamed, and H. Arshad, "State-of-the-art in artificial neural network applications: A survey," Heliyon, vol. 4, no. 11, p. e00938, 2018, doi: 10.1016/j.heliyon.2018.e00938.
[50] D. N. Ganesan, D. K. Venkatesh, D. M. A. Rama, and A. M. Palani, "Application of Neural Networks in Diagnosing Cancer Disease using Demographic Data," Int. J. Comput. Appl., Volume 1, No. 26, pp. 81–97, 2010, doi: 10.5120/476-783.
[51] R. R. Sarra, A. M. Dinar, and M. A. Mohammed, "Enhanced accuracy for heart disease prediction using artificial neural network," Indones. J. Electr. Eng. Comput. Sci., Volume. 29, No. 1, pp. 375–383, 2023, doi: 10.11591/ijeecs.v29.i1.pp375-383.
[52] L. A. Al-Haddad and A. A. Jaber, "An Intelligent Fault Diagnosis Approach for Multirotor UAVs Based on Deep Neural Network of Multi-Resolution Transform Features," Drones, Volume 7, No. 2. p. 82, 2023. doi: 10.3390/drones7020082.
[53] S. Mohapatra and T. Swarnkar, "Comparative Study of Different Orange Data Mining Tool-Based AI Techniques in Image Classification," in Lecture Notes in Networks and Systems, vol. 202 LNNS, Springer, 2021, pp. 611–620. doi: 10.1007/978-981-16-0695-3_57.
[54] H. M and S. M.N, "A Review on Evaluation Metrics for Data Classification Evaluations," Int. J. Data Min. Knowl. Manag. Process, Volume 5, No. 2, pp. 01–11, 2015, doi: 10.5121/ijdkp.2015.5201.

ИНОВАТИВНА ПРИМЕНА ВЕШТАЧКИХ НЕУРОНСКИХ МРЕЖА ЗА ЕФИКАСНУ ЛОКАЛИЗАЦИЈУ ПРСЛИНА РОТАЦИОНОГ ВРАТИЛА

С.М. Шакир, А.А. Џабер

Ротациона вратила су кључне компоненте у индустријским окружењима и одговорне су за пренос обртног момента и ротационог кретања. Упркос свом значају, ове осовине су подложне кваровима, посебно напрслинама, које могу негативно утицати на перформансе и безбедност система. Стога, ефикасно откривање и дијагностика пукотина осигуравају сигурност, поузданост и економичност. Ово истраживање има за циљ да развије модел вештачке неуронске мреже (АНН) који може ефикасно да идентификује пукотине које се јављају на различитим дубинама и на различитим локацијама у ротирајућим вратилима, које раде при различитим брзинама ротације. Сигнали вибрације су добијени и подвргнути претходној обради коришћењем пропусног филтера да би се изоловали сигнали осовине од других компоненти. Након тога, статистичке карактеристике временског домена су издвојене из филтрираних сигнала. Оптимална методологија одабира карактеристика је коришћена за рангирање издвојених карактеристика, а карактеристике највишег ранга су изабране за обуку модела АНН. Налази овог истраживања указују да је развијени модел постигао тачност класификације од 94,4%.